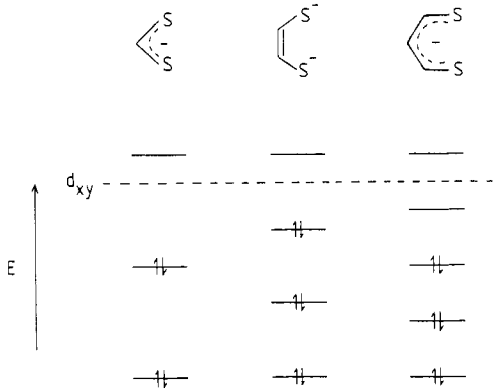

Figure 12. Qualitative π-molecular orbital energy level diagram for 1,1-, 1,2-, and 1,3-dithio ligands.

reason for this can be seen from a qualitative π-molecular orbital energy level diagram for the ligands (Figure 12). The increasing degree of conjugation from the 1,1- to the 1,3-dithiolate ligand results in a lowering in energy of the π-antibonding orbitals to the point where one of these becomes more stable than the lowest energy σ-antibonding metal orbital involving the d_{xy} orbital. It is interesting to note that essentially the same diagram as Figure 12 was used by Schrauzer to account for the observation that a range of oxidation states are accessible for complexes of "even" (1,2-dithio) ligands, but not for complexes of "odd" (1,1- or 1,3-dithio) ligands.[30] This argument applies only to oxidation reactions of complexes of the ligands in the oxidation states shown in Figure 12, however. It is now clear that one-electron-reduction reactions are possible in all three cases, but only in the case of the 1,3-dithio ligand do the π-orbital energies become low enough to allow ligand-centered (rather than metal-centered) reductions to take place.

One as yet unexplained feature of this model in relation to the complexes studied in the present work is that it does not seem to apply to mixed-ligand complexes such as $[Ni(SacSac)(dpe)]^+$, whose one-electron reduction is found to be essentially metal based. The possibility that additional stabilization of the ligand π orbitals in $Ni(SacSac)_2$ occurs through interaction between orbitals on the different ligands can be ruled out because the π orbitals of the complex all occur as near-degenerate pairs. Thus, there must be a lowering of the energy of the metal d orbitals in $[Ni(SacSac)(dpe)]^+$ relative to $Ni(SacSac)_2$, although the reason for this is not clear at present.

The stabilization of the (a_u, b_{2g}) ligand antibonding π orbitals relative to 1,1- and 1,2-dithio ligand complexes may be understood in terms of the stabilizing π-bonding interaction between the sulfur ligand atom and the ajacent carbon atom and the weaker antibonding interaction between these carbon-sulfur π-bonding orbitals due to the presence of the extra methene carbon in the 1,3 ligand (Figure 7). In the case of the 1,2 ligand these orbitals are raised in energy due to the stronger antibonding interaction between the adjacent 1,2-carbon atoms.[27]

Acknowledgment. We thank Janet Hope for some preliminary experiments on $Ni(SacSac)_2$ and Professor R. L. Martin for his interest in this problem. We also thank Dr. Michael Cook for a copy of the Xα-SW programs used in this study.

Registry No. $[Ni(SacSac)_2]$, 64705-81-3; $[Ni(t\text{-}BuSac\text{-}t\text{-}BuSac)_2]^-$, 61024-06-4; $[Ni(CH_2{=}CHCH_2SacSac)_2]^-$, 93304-99-5; $[Ni(CF_3SacSac)_2]^-$, 93280-88-7; $[Ni(NorSacSac)_2]^-$, 93280-89-8; $[Pd(SacSac)_2]^-$, 93280-90-1; Ni(SacSac)(dpe), 93280-91-2; Ni(*t*-BuSac-*t*-BuSac)(dpe), 93280-92-3.

(30) Schrauzer, G. N. *Acc. Chem. Res.* **1969**, *2*, 72.

Contribution from the Centre de Recherches Nucléaires, 67037 Strasbourg Cedex, France, Institut für Anorganische Chemie der Universität, Karlsruhe, Federal Republic of Germany, and Kamerlingh Onnes Laboratorium, Rijks Universiteit, Leiden, The Netherlands

Structural, Magnetic, and Electronic Properties of Europium Dihalides, EuX_2 (X = Cl, Br, I)

J. P. SANCHEZ,*† J. M. FRIEDT,† H. BÄRNIGHAUSEN,‡ and A. J. VAN DUYNEVELDT§

Received March 15, 1984

Structural, magnetic, and ^{151}Eu Mössbauer hyperfine interaction data are reported for the europium dihalides $EuCl_2$, $EuBr_2$, and EuI_2. The linear correlation observed between the isomer shift and the saturation hyperfine field indicates changing bonding ionicity, with the determinant result of increasing 6s charge and spin density with decreasing ionicity. The electronic structure and magnetic superexchange mechanisms in the dihalides are discussed and compared to those in other Eu^{2+} compounds.

Introduction

Considerable effort has been devoted over the last decade to the elucidation of the electronic and magnetic properties of divalent europium insulators or semiconductors, in particular from the hyperfine interaction parameters.[1] Most of this activity dealt with the europium monochalcogenides, with emphasis on the ferromagnetic semiconductors EuO and EuS, which are model systems for the Heisenberg exchange interactions.[2] The magnetic exchange mechanism in these materials has been analyzed thoroughly by Kasuya:[3] direct overlap and mixing of 4f and 5d orbitals between nearest-neighbor Eu^{2+} ions (nn) allows for a ferromagnetic nn exchange (J_1) whereas superexchange via anion p orbitals provides a mostly antiferromagnetic next-nearest-neighbor (nnn) coupling (J_2).

The Mössbauer isomer shift (δ_{IS}) measures the charge density at the nucleus whereas the hyperfine field (H_{hf}) reflects the spin density. Hence, if these two parameters originate from the same electrons, a linear correlation between δ_{IS} and H_{hf} is predictable in a series of chemically comparable compounds. A monotonous correlation has indeed been reported in several intermetallic alloys and is understandable under the condition of a conduction band of predominantly s character.[4,5] It is of particular interest to check

† Centre de Recherches Nucléaires.
‡ Universität Karlsruhe.
§ Rijks Universiteit.

(1) Bauminger, E. R.; Kalvius, G. M.; Nowik, I. In "Mössbauer Isomer Shifts"; Shenoy, G. K., Wagner, F. E., Eds.; North-Holland Publishing Co.: Amsterdam, 1978; Chapter 10, p 663.
(2) For recent reviews see: Wachter, P. In "Handbook on the Physics and Chemistry of Rare Earths"; Gschneidner, K. A., Jr.; Eyring, L., Eds.; North-Holland Publishing Co.: Amsterdam, 1979; Vol. II, Chapter 19, p 507. Holtzberg, F.; von Molnar, S.; Coey, J. M. D. In "Handbook of Semiconductors"; Keller, S. P., Ed.; North-Holland Publishing Co.: Amsterdam, 1980; Vol. III, p 803.
(3) Kasuya, T. *IBM J. Res. Dev.* **1970**, *14*, 214.
(4) Nowik, I.; Dunlap, B. D.; Wernick, J. H. *Phys. Rev. B: Solid State* **1973**, *8*, 238.

0020-1669/85/1324-0408$01.50/0

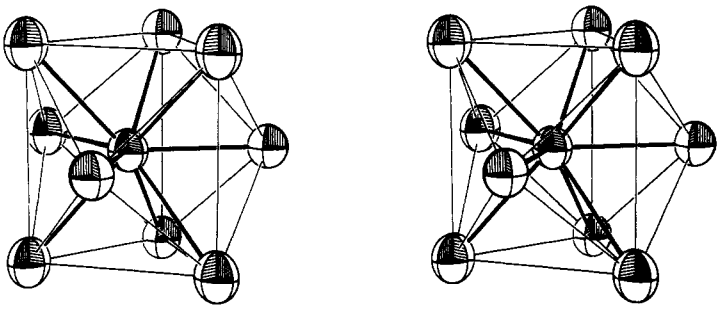

Figure 1. Coordination polyhedron of Eu in $EuCl_2$ (site symmetry C_s).

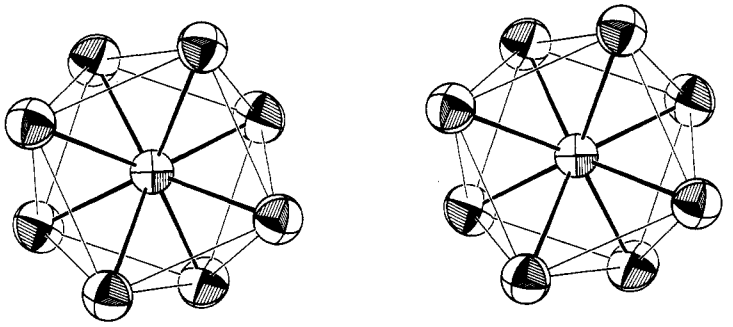

Figure 2. Coordination polyhedron of Eu(1) in $EuBr_2$ (site symmetry C_4).

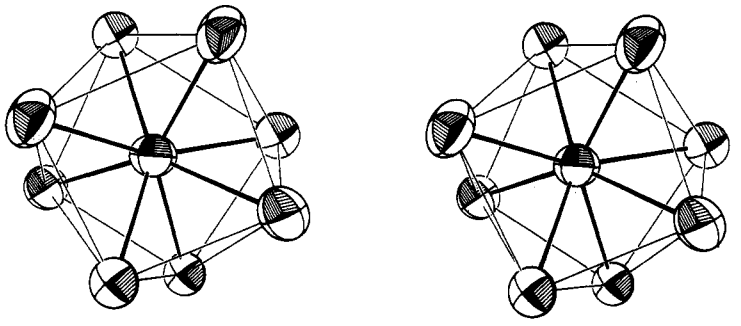

Figure 3. Coordination polyhedron of Eu(2) in $EuBr_2$.

for the possible occurrence of a similar correlation in insulating compounds: such systems might be better suited to semitheoretical discussion based on empirical concepts of chemical bonding.

Little thorough attention has been paid until now to the physical properties of Eu^{2+} halides, EuX_2 (X = Cl, Br, I), primarily owing to difficulties of preparation and of handling. The few magnetic data already published should be considered with caution.[6] Indeed, the ferromagnetic and paramagnetic behavior (at 4.2 K) reported for EuI_2 and $EuBr_2$, respectively, must probably be attributed to ill-defined compounds, possibly monohydrates, $EuX_2 \cdot H_2O$.[7] The present work concentrates on the magnetic and bonding properties of well-characterized EuX_2 samples for which detailed crystallographic data have been worked out.[8-11] It is found consistently from ac susceptibility (χ_{ac}) and Mössbauer measurements that $EuCl_2$ and EuI_2 order magnetically in a range between 1.6 and 1.8 K whereas $EuBr_2$ remains paramagnetic down to 1.1 K. The nature of the magnetic order in $EuCl_2$ and EuI_2 is established by the χ_{ac} behavior. The variation of δ_{IS} and H_{hf} (measured by ferromagnetic alignment of the Eu^{2+} spins under a large external field at 4.2 K) along the halide series is discussed in terms of bonding properties. It is shown that the covalency effects proceed primarily via charge transfer from the ligands s (p) orbitals to the empty Eu 6s orbital.

Table I. Crystallographic Data for the Europium Dihalides

compd	cryst syst, space group, Z	lattice const[a]
$EuCl_2$	orthorhombic, *Phnm* (No. 62), 4	a = 8.963 (1) Å b = 7.536 (1) Å c = 4.5087 (5) Å
$EuBr_2$	tetragonal, $P4/n$ (No. 85); 10	a = 11.563 (3) Å c = 7.091 (2) Å
EuI_2	monoclinic, $P2_1/c$ (No. 14), 4	a = 7.622 (2) Å b = 8.246 (2) Å c = 7.894 (2) Å β = 98.02 (2)°

[a] Standard deviations in parentheses.

Experimental Section

Preparation of Compounds.[12] The europium dihalides, EuX_2 (X = Cl, Br, I), were obtained by carefully controlled thermal dehydration and decomposition of the corresponding trihalide hexahydrates, $EuX_3 \cdot 6H_2O$, under high vacuum. The samples were purified by high-vacuum distillation. The europium dihalides are highly moisture and air sensitive,

(5) van Steenwijk, F. J. Thesis, University of Leiden, 1976 (unpublished).
(6) McGuire, T. R.; Shafer, M. W. *J. Appl. Phys.* **1964**, *33*, 984.
(7) "Gmelins Handbook of Inorganic Chemistry", 8th ed.; Springer-Verlag: Berlin, 1978; Vol. 39-C6, pp 69, 195.
(8) Bärnighausen, H.; Schultz, N. *Acta Crystallogr., Sect. B: Struct. Crystallogr. Cryst. Chem.* **1969**, *B25*, 1104.
(9) Bärnighausen, H. *Rev. Chim. Miner.* **1973**, *10*, 77.
(10) Bärnighausen, H.; Beck, H. P.; Grueninger, H. W. *Proc. Rare Earth Res. Conf.* **1971**, *9*, 74.
(11) Beck, H. P. Dissertation, Universität Karlsruhe, 1972 (unpublished).
(12) Brauer, G. "Handbuch der Präparativen Anorganischen Chemie", 3rd ed.; Enke Verlag: Stuttgart, 1978; Vol. II, pp 1074–84.

Table II. Positional Parameters for the Europium Dihalides from Single-Crystal Structure Determinations

compd	ref	atom	Wyckoff posn	site sym	x	y	z
$EuCl_2$	9	Eu	4(c)	m	0.11510 (3)	0.24952 (3)	0.25
		Cl(1)	4(c)	m	0.42788 (12)	0.14342 (13)	0.25
		Cl(2)	4(c)	m	−0.16675 (14)	0.02379 (15)	0.25
$EuBr_2$	10, 11	Eu(1)	2(c)	4	0.25	0.25	0.3555 (3)
		Eu(2)	8(g)	1	0.1030 (1)	0.5871 (1)	0.7489 (1)
		Br(1)	8(g)	1	0.1610 (2)	0.0424 (2)	0.6026 (3)
		Br(2)	8(g)	1	0.0395 (2)	0.1554 (2)	0.1256 (3)
		Br(3)	2(b)	$\bar{4}$	0.25	0.75	0.50
		Br(4)	2(a)	$\bar{4}$	0.25	0.75	0
EuI_2	8	Eu	4(e)	1	0.21375 (13)	0.44728 (12)	0.30521 (28)
		I(1)	4(e)	1	0.40093 (18)	0.10933 (18)	0.21577 (38)
		I(2)	4(e)	1	−0.07653 (16)	0.26998 (16)	−0.00487 (31)

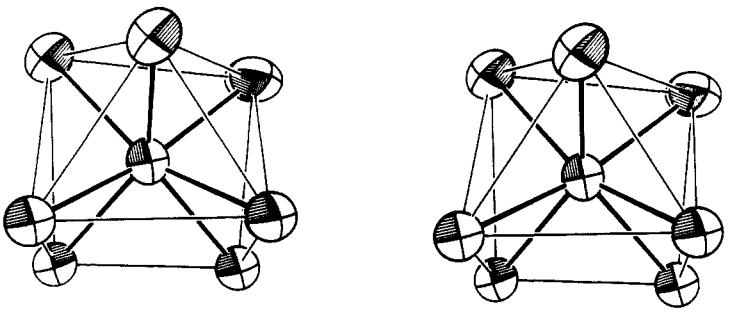

Figure 4. Coordination polyhedron of Eu in EuI_2.

requiring transfer and handling in a glovebox under dried argon.

X-ray Diffraction.[8-11] The lattice parameters and the structural assignment of the samples have been established by X-ray powder diffraction using a Guinier camera modified to handle air-sensitive compounds.[13] The film readings were made with a coincidence micrometer, and the measured values were calibrated with the diffraction lines of Si (a_0 = 5.43094 Å), which was employed as an internal standard. With a least-squares program, refined lattice parameters have been obtained (Table I). Especially for EuI_2 there is a considerable improvement with respect to earlier data. It is convenient to summarize the positional parameters of the europium dihalides (Table II) and to give a rough description of their crystal structures including relevant interatomic distances.

$EuCl_2$ crystallizes with the $PbCl_2$-type structure.[9] The Eu^{2+} ion is surrounded by nine Cl^- ions (7 + 2 coordination). The Eu–Cl distances range from 2.915 to 3.439 Å with a mean value of 3.095 Å. A stereoscopic drawing of the coordination polyhedron, a so-called tricapped trigonal prism, is shown in Figure 1.

$EuBr_2$ crystallizes with the $SrBr_2$-type structure.[10,11] There are two crystallographically different Eu^{2+} positions in this structure, but both are eightfold coordinated by Br^- ions. The coordination polyhedron of Eu(1) is an almost regular square antiprism, as can be seen from Figure 2. In contrast, the Eu(2) polyhedron is highly distorted (7 + 1 coordination), but again the similarity with a square antiprism is evident (see Figure 3). Eu(1) has four Br^- neighbors at 3.127 Å and four at 3.145 Å (mean value 3.136 Å). The Eu(2)–Br distances range from 3.091 to 3.517 Å with a mean value of 3.190 Å.

EuI_2 has its own structure type[8] that is closely related to the monoclinic modification of ZrO_2 (baddeleyite). The Eu^{2+} ion is surrounded by seven I^- ions between 3.252 and 3.393 Å (mean Eu–I distance 3.337 Å). Geometrical details of the coordination polyhedron (called tetragonal base–trigonal base) can be seen from Figure 4. In this and the other stereoscopic drawings[14] the thermal vibration ellipsoids are shown on the 99% probability level.

Magnetic Measurements. The dc magnetic susceptibility (4.2–300 K) was measured by a Faraday balance system (Oxford Instruments) at a field of 10.5 kOe and a gradient of 100 Oe/cm. The ac susceptibility (1.1–4.2 K) was measured by using a mutual inductance technique. Both the in-phase (χ') and out of phase (χ'') susceptibility were recorded simultaneously with a two-phase lock-in amplifier.[15] The absolute susceptibility calibration is performed by reference to the standard paramagnet $Mn(NH_4)_2(SO_4)_2 \cdot 6H_2O$.

Table III. Mössbauer Parameters of the Europium Dihalides at 77 K[a]

	δ_{IS}, mm/s	e^2q_zQ, mm/s	η	W, mm/s
EuF_2	−13.36 (10)	~0		
$EuCl_2$	−13.16 (2)	−8.3 (3)	0.87 (8)	2.84 (7)
	−13.19 (2)	+8.1 (3)	0.9 (1)	2.85 (7)
$EuBr_2$	−13.09 (3)	+8.8 (5)	0.6 (1)	2.75 (12)
EuI_2	−12.70 (3)	−5.8 (2)	0.8 (2)	2.45 (10)
	−12.73 (2)	+6.3 (4)	0.76 (12)	2.40 (10)

[a] δ_{IS} is the isomer shift given with respect to the SmF_3 source at 77 K. e^2q_zQ is the quadrupole coupling constant (1 mm/s = 17.4 MHz). η is the asymmetry parameter and W the line width of the 12-line quadrupolar pattern. The isomer shift of EuF_2 is estimated from ref 16 by taking $\Delta\delta_{IS}(EuF_2 - EuCl_2) = -0.2$ mm/s.

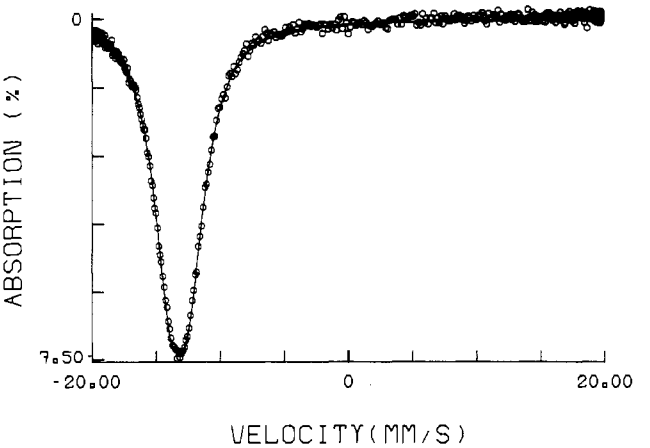

Figure 5. ^{151}Eu Mössbauer spectrum of $EuCl_2$ at 77 K. The solid line is the fitted curve assuming e^2q_zQ negative (see text).

^{151}Eu Mössbauer Measurements. The measurements were performed with the samples mounted in tight aluminum holders with indium seals, using the 21.6-keV resonance of ^{151}Eu, on natural europium absorbers of 5–10 mg of ^{151}Eu/cm^2. The source of $^{151}SmF_3$ (300 mCi) is moved, with the velocity changing as a sinus function of time, in synchronization with a multichannel analyzer operating in time mode. Temperatures between 1.5 and 4.2 K were controlled by pumping on the helium bath

(13) Simon, A. *J. Appl. Crystallogr.* **1970**, *3*, 11.
(14) Johnson, C. K. "ORTEP II", Report ORNL-3794 (Revised Version); Oak Ridge National Laboratory: Oak Ridge, TN, 1971.
(15) Groenendijk, H. A.; van Duyneveldt, A. J.; Willett, R. D. *Physica B+C (Amsterdam)* **1980**, *101*, 320.
(16) Ehnholm, G. J.; Katila, T. E.; Lounasmaa, O. V.; Reivari, P.; Kalvius, G. M.; Shenoy, G. K. *Z. Phys.* **1970**, *235*, 289.

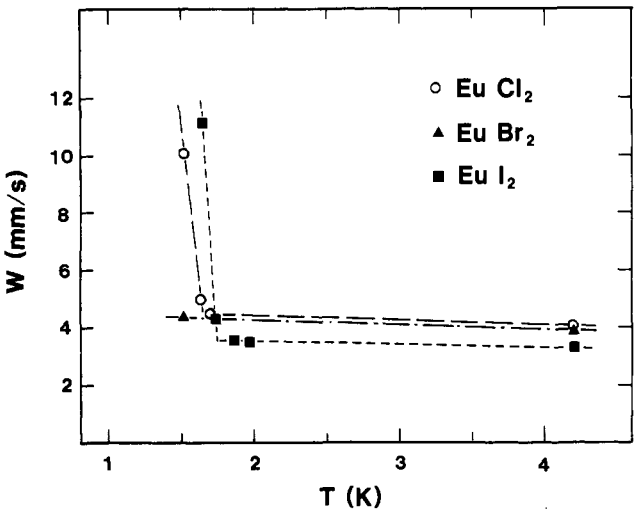

Figure 6. Temperature dependence of the resonance line width (W). The abrupt change of $W(T)$ represents the onset of magnetic order.

through a manostat. Some experiments were carried out in a longitudinal (i.e., parallel to the γ beam) magnetic field of 80 kOe provided by a superconducting magnet. The experimental data were computer least-squares analyzed directly for the hyperfine parameters by constraining the relative energies and intensities of the Lorentzian lines to the theoretical values. In the case of combined quadrupole and magnetic interactions, the calculation of the spectral shape is performed by diagonalization of the full nuclear Hamiltonian as discussed in more detail in the next section.

Experimental Results

1. Mössbauer Spectroscopy. (a) Zero External Field Measurements. At 77 and 4.2 K the Mössbauer spectra of the three halide samples EuX_2 (X = Cl, Br, I) consist of a broadened resonance line (pseudo single line width ranging from 3.3 to 4.1 mm/s at 4.2 K) with an isomer shift characteristic of Eu^{2+} (Figure 5; Table III). The onset of magnetic ordering in $EuCl_2$ and EuI_2 is established from the temperature dependence of the resonance width: this is almost constant down to the magnetic transition temperature (T_t = 1.64 (5) and 1.75 (5) K for $EuCl_2$ and EuI_2, respectively), below which it diverges sharply (Figure 6). $EuBr_2$ remains paramagnetic down to the lowest temperature (1.5 K) attainable with our experimental set up.

The line broadenings observed in the paramagnetic phase of the europium dihalides arise from unresolved quadrupolar effects, consistent with the low symmetry of the Eu^{2+} sites (see crystallographic data). It has been pointed out that the derivation of the hyperfine interaction parameters from unresolved quadrupole spectra can give rise to errors when thick absorbers are used[17] (i.e., whenever $t_a = n\sigma_0 f_a > 2$, where n is the specific number of resonant atoms, σ_0 the resonance cross section, and f_a the Debye–Waller factor). In order to avoid possible errors connected with intensity saturation effects, the analysis of paramagnetic hyperfine data is limited to measurements recorded at 77 K (Table III; Figure 5). In both $EuCl_2$ and EuI_2, the asymmetry parameter (η) of the electric field gradient (EFG) tensor is close to unity. This prevents a reliable determination of the sign of the principal component (eq_z) from paramagnetic data. However, ultralow-temperature Mössbauer measurements in the ordered phase of $EuCl_2$[16] (e^2q_zQ = −8.3 (9) mm/s) as well as ESR data on Eu^{2+}:$PbCl_2$[18] ($EuCl_2$ is isostructural with $PbCl_2$; e^2q_zQ = −5.6 (20) mm/s, η = 0.7 (2)) demonstrate that e^2q_zQ is negative in $EuCl_2$. For EuI_2, the undetermination of the sign of e^2q_zQ does not affect significantly the actual value for the isomer shift, which is hence measured with reasonable precision (Table III). In $EuBr_2$, the Eu^{2+} ions occupy two different crystallographic sites. The poor resolution of the quadrupole pattern does not allow resolution of several subspectra; hence, only average values for the hyperfine interaction parameters can be derived.

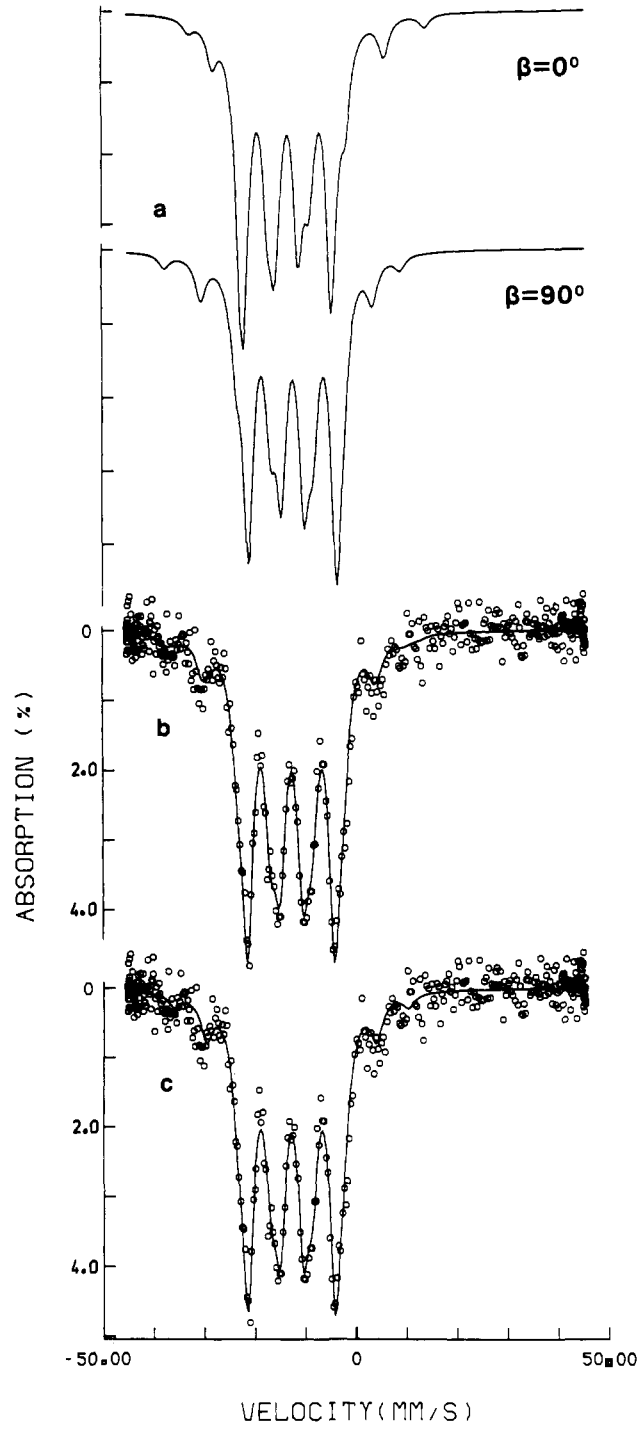

Figure 7. (a) Mössbauer spectra computed with the electrostatic hyperfine parameters measured in $EuCl_2$ at 77 K (δ_{IS} = −13.16 mm/s, e^2q_zQ = −8.3 mm/s, η = 0.9) for an effective field of (−)226 kOe and on the assumption of full polarization of the magnetic moment along the direction of propagation of the γ rays. The two figures correspond to q_z being respectively parallel (β = 0) and perpendicular (β = 90) to H_{eff}. (b) Experimental spectrum of $EuCl_2$ at 4.2 K in an external field of 80 kOe parallel to the $\vec{k}$ vector. The solid line corresponds to a fit with random orientation between H_{eff} and q_z (e^2q_zQ = −8.3 mm/s, η = 0.9) and moment polarization along $\vec{k}$. (c) Same experimental result as in (b). The fit (solid line) includes zero quadrupole interaction and polarization of H_{eff} along the $\vec{k}$ vector.

(b) Saturation Hyperfine Field at ^{151}Eu in EuX_2 from External Field Measurements. The saturation hyperfine field, H_{hf}^s, cannot be reliably determined in the ordered state of the compounds EuX_2 under our experimental conditions since the lowest achievable measuring temperature (1.5 K) is too close to the ordering tem-

(17) Shenoy, G. K.; Friedt, J. M.; Maletta, H.; Ruby, S. L. In "Mössbauer Effect Methodology"; Gruverman, I. J., Seidel, C. W., Kieterly, D. K., Eds.; Plenum Press: New York, 1974; Vol. 9, p 277.

(18) Vrehen, Q. H. F.; Volger, J. *Physica (Amsterdam)* **1965**, *31*, 845.

Table IV. Magnetic Transition Temperature and Saturation ^{151}Eu Hyperfine Field of Europium Dihalides As Deduced from Mössbauer Measurements

compd	T_t, K	H_{hf}^s, kOe	compd	T_t, K	H_{hf}^s, kOe
EuF_2	1.0 (1)[a]	(−)333 (3)[a]	$EuBr_2$		(−)305 (5)
$EuCl_2$	1.64 (5)	(−)313 (3)	EuI_2	1.75 (5)	(−)291 (3)

[a] Reference 16.

peratures. Hence, a safe extrapolation to saturation conditions implies very precise knowledge of transition and measuring temperatures as well as the actual temperature dependence of the hyperfine field (close to T_t, the use of a Brillouin function is questionable owing to the possible occurrence of relaxation effects). Therefore, the precise evaluation of H_{hf}^s is performed in the paramagnetic phase, using polarization by an intense external field (Figure 7). The effective field acting at the ^{151}Eu nucleus is the sum of the applied field (H_{app}) and of the internal hyperfine field H_{hf}. The saturation field H_{hf}^s is evaluated straightforwardly by assuming free-ion Brillouin behavior for H_{hf} (the exchange contribution being negligible):

$$H_{eff} = H_{app} + H_{hf}^s \mathcal{B}_{7/2}(7\mu_B H_{app}/k_B T) \quad (1)$$

Under present experimental conditions, $T = 4.2$ K and $H_{app} = 80$ kOe, 98% of the saturation value is reached. The effective field is negative, i.e., antiparallel to the applied field, as deduced from the field dependence of H_{eff} and consistent with the negative sign of the core polarization field that represents the main contribution to H_{hf}.

The theoretical analysis of such magnetically perturbed paramagnetic data requires special caution connected with the occurrence of the EFG at the nucleus: indeed, the electronic moment (and consequently the hyperfine field of the S-state Eu^{2+} nuclei) is aligned along the large external field. Since polycrystalline samples are used, the EFG principal axis is at a random orientation with respect to H_{app}. Therefore, a strict analysis must consider the resulting polarization and distribution of the polar (β) and azimuthal (φ) angles between the EFG and H_{eff} axes. This is done numerically (Figure 7b) but is highly computer time consuming because of the large values of the nuclear spins involved in the ^{151}Eu resonance ($I_g = {}^5/_2$, $I_e = {}^7/_2$). Alternatively, the quadrupole interaction may be treated as a perturbation of the magnetic hyperfine interaction so that the nuclear Hamiltonian interaction reduces to

$$\mathcal{H}_N = -g_I\mu_N\hat{I}_z H_{eff} + [e^2q_zQ/8I(2I-1)] \times [3\hat{I}_z^2 - I(I+1)][(3\cos^2\beta - 1) + \eta\sin^2\beta\cos(2\varphi)] \quad (2)$$

For a uniform distribution of the angles β and φ, the angular average of the last term in brackets (eq 2) vanishes to zero, hence inducing an effective cancellation of the effect of the quadrupole interaction.[19] Second-order perturbation predicts nonuniform line broadening.[20] However, such a treatment is of little interest because of the practical overlap of the resonance components (Figure 7). We have checked numerically that H_{eff} is fitted safely when neglecting the quadrupole interaction and allowing merely for a uniform line broadening (compare Figure 7b,c). The above approximation appears only as a slight misfit in the widths of the outer resonance peaks. The saturated hyperfine fields deduced for the series of the Eu dihalides are presented in Table IV. Notice that the H_{hf}^s value of (−)313 kOe found for $EuCl_2$ is in good agreement with the one that was formerly determined, (−)315 (3) kOe, in the ordered phase using a dilution refrigerator.[16]

2. Dc and Ac Susceptibility Data. The dc susceptibility of the Eu dihalides (sealed in quartz ampules under helium exchange gas) has been measured on a Faraday balance at temperatures between 4.2 and 300 K. The dc susceptibilities are corrected for the diamagnetism of the ionic cores according to values given by Selwood.[21] They obey a Curie law, indicating weak magnetic interactions. The effective paramagnetic moments evaluated from the Curie slope are perfectly consistent with the theoretical Eu^{2+} free-ion value of 7.94 μ_B (Table V).

Table V. Magnetic Data for Europium Dihalides[a]

compd	μ_{eff}, μ_B	Θ, K	T_t, K
$EuCl_2$	7.83 (4)	0 (1)	1.60 (2)
$EuBr_2$	7.86 (4)	0 (1)	
EuI_2	7.94 (4)	0 (1)	1.76 (2)

[a] The effective paramagnetic moment μ_{eff} and the paramagnetic Curie temperature Θ are as deduced from high-field χ_{dc} measurements. The ordering temperatures T_t are those obtained from low-field χ_{ac} measurements.

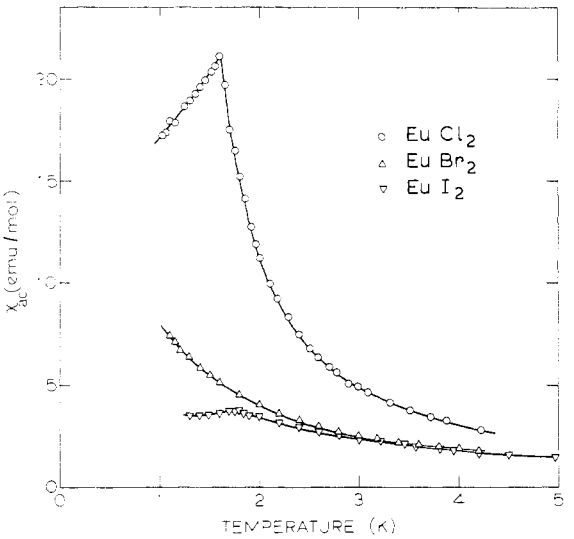

Figure 8. Temperature dependence of the ac magnetic susceptibility of $EuCl_2$, $EuBr_2$, and EuI_2.

The ac susceptibility measurements have been performed in order both to extend the analysis of magnetic properties down to 1 K and to establish the types of ordering. The measurements performed at a frequency of 234 Hz are included in Figure 8. The largest susceptibility is measured for $EuCl_2$. Magnetic ordering is clearly detected at 1.60 (2) K. It is deduced to be ferromagnetic from the observation of a large signal. Owing to the polycrystalline nature of the sample, it is impossible to estimate whether the maximum value of χ_{ac} reaches the reciprocal demagnetizing limit. As expected for a ferromagnet in zero external field, the onset of out-of-phase signals is observed below T_t and assigned to domain wall relaxation.[22] An external field of a few kilooersted is sufficient to align the ferromagnetic moments, as shown by vanishing susceptibility at 4 kOe.

For $EuBr_2$, the absence of ordering down to 1.1 K is clear from Figure 8. However, the results suggest the possibility of a ferromagnetic ordering below this temperature.

For EuI_2, the magnetic transition occurring at 1.76 (2) K is tentatively assigned to antiferromagnetism from both the decreased susceptibility in comparison to $EuCl_2$ and the absence of out-of-phase signal below T_t. Single-crystal studies are necessary in order to elucidate fully the type of ordering of EuI_2.

Discussion

1. Electronic Charge and Spin Densities. The electronic charge density at the nucleus, $\rho(0)$, which is measured from δ_{IS}, corresponds to the summed projection from the atom's s and $p_{1/2}$ orbitals. In Eu compounds, $\rho(0)$ will directly reflect the change of population of the valence 6s orbital and indirectly the change in the non-s (4f, 5d) valence orbitals. The latter exert a shielding

(19) Nam Ok, H.; Morrish, A. H. *Phys. Rev. B: Condens. Matter* **1980**, *22*, 4215.
(20) See e.g.: Bonnenfant, A.; Friedt, J. M.; Maurer, M.; Sanchez, J. P. *J. Phys. (Orsay, Fr.)* **1982**, *43*, 1475.
(21) Selwood, P. W. "Magnetochemistry"; Interscience: New York, 1956; p 78.
(22) Groenendijk, H. A.; van Duyneveldt, A. J. *Physica B+C (Amsterdam)* **1982**, *115*, 41.

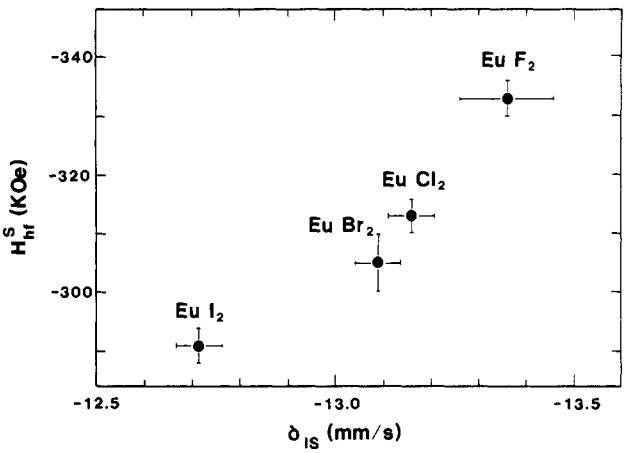

Figure 9. Correlation between the isomer shift (δ_{IS}) and the saturation hyperfine field (H_{hf}^{s}) for the europium dihalides.

effect on the core and valence (s, $p_{1/2}$) electrons that can be estimated by reference to free-ion electron density calculations:[1,23] the shielding produced by one 5d electron represents approximately 30% of one 4f electron. The change of $\rho(0)$ produced by one 6s electron is comparable (and of opposite sign) to the effect of one 4f electron. In an actual solid, where the Eu atom will present an electron configuration $4f^n5d^16s^m$, $\rho(0)$ can be discussed as first order by assuming a linear interpolation between free-ion electron densities.

The hyperfine field acting at the Eu^{2+} nucleus is composed of a sum of several contributions:[4,24]

$$H_{hf} = H_{CP} + H_{OP} + H_{TR} + H_{DIP} \quad (3)$$

H_{CP} is defined as the contribution due to the core s orbitals, which are spin-exchange polarized by the open 4f shell. Inasmuch as the 4f electron density is unaffected by chemical bonding, this term is a constant that is evaluated to −340 kOe from ENDOR results of Eu^{2+}:CaF_2.[25] H_{OP} arises from the spin polarization of the valence (6s, 5d) orbitals by the 4f spin. The field produced by one unpaired 6s electron is positive and amounts of 7.5×10^3 kOe whereas the field produced by one 5d electron is negative and an order of magnitude smaller.[26] H_{TR} is the transferred field due to neighboring Eu ions. In view of the very low magnetic transition temperatures found in the Eu dihalides, it is safe to assume that the latter contribution (H_{TR}) is negligibly small. Also, the effective dipolar field (H_{DIP}) is estimated to be negligibly small. Thus, expression 3 reduces to the two first contributions. The term H_{OP} will represent the changes of electronic structure of the europium atom as a result of chemical bonding. It is predicted to be correlated to the isomer shift since these two parameters are respectively proportional to the electronic spin and charge densities at the nucleus. A linear correlation is observed indeed between δ_{IS} and H_{hf} for the series of dihalides under consideration (Figure 9).

In the absence of electron density calculations from molecular orbital techniques, it is of interest to consider the possibility of an empirical discussion of bonding properties from the experimental correlation δ_{IS} vs. H_{hf}^{s} (Figure 9). The monotonous decrease of $|\delta_{IS}|$ from EuF_2 to EuI_2 indicates an increase of $\rho(0)$ in this order (Table III), i.e. either an increase of the population of the 6s valence orbital or (and) a decrease of the valence 5d orbital occupation. The participation of 5d electrons to bonding can be argued to be negligible; this is revealed for instance from their minor contribution to magnetic exchange, which is indicated by the low ordering temperatures observed in the dihalides in comparison to, e.g., the chalcogenides.[27] Also, the evolution of the saturation hyperfine field $|H_{hf}^{s}|$ along the series of compounds is consistent with an enhanced exchange polarization of the 6s valence orbital from the fluoride to the iodide; indeed, the polarization of the 6s charge density by the 4f spin provides a positive contribution to H_{hf}, i.e. antiparallel to the major core polarization field H_{CP} (of negative sign). Therefore, an increasing population in the 6s orbital will induce a decreasing modulus for H_{hf}^{s}.

It has often been found possible to correlate the Mössbauer isomer shift with the ligand electronegativity in homogeneous series of compounds with constant coordination geometry.[28,29] The result is understandable since this parameter expresses the extent of the ionicity of interatomic bonding and hence the degree of electron charge transfer between the two constituent ions. A linear relationship is indeed observed between both δ_{IS} and H_{hf}^{s} and the halogen electronegativity[30] (Figure 10a) (in spite of different metal coordinations in the compounds under consideration; see Experimental Section).

An alternative empirical correlation worth considering involves the ligand polarizability, which may provide a more adequate representation of the degree of exchange of charge density in the solid state.[31] A linear relationship is indeed observed between this parameter and the hyperfine parameters δ_{IS} and H_{hf}^{s} (Figure 10b).

Hence, it seems safe to conclude an increasing electron charge transfer from the ligand onto the Eu^{2+} ion in the sequence from the fluoride to the iodide. The evolution of the hyperfine parameters δ_{IS} and H_{hf}^{s} reveals that this transfer involves determinantly the 6s valence orbital of Eu, the effects implying other orbitals (5d, possibly 4f) being undetectable.

The simple covalency mechanism developed above in order to represent the observed linear correlation between δ_{IS} and H_{hf}^{s} in the Eu dihalides (in terms of determinant effect of 6s covalency effect) cannot be extrapolated to the Eu chalcogenides. In the latter series of compounds, the slope of the correlation between δ_{IS} and covalency is of sign opposite to the one in the dihalides whereas no clear relationship appears between H_{hf}^{s} (corrected for different magnetic structures) and covalency.[32] This behavior is reasonably assigned to different bonding mechanisms as connected with the widely different interatomic distances and site symmetries. Hence, in the chalcogenides, the contribution of 5d covalent mixing might conceivably overwhelm the effect of 6s shell transfer[32] and thus cancel the simple relationship observed in the halides.

2. Local Structural Information. The EFG tensor arises merely from the lattice contribution in view of the spherically symmetrical electron charge distribution for an Eu^{2+} (^8S) ion. Except in EuF_2[16,33] (Eu site of cubic symmetry), the Eu^{2+} ions occupy lattice sites of symmetry lower than axial, consistent with the large values measured for eq_z and η (Table III). A calculation of the lattice EFG[18] has not been attempted. However, it is worth noticing the good agreement between the presently determined EFG parameters in $EuCl_2$ and those reported from ESR for Eu^{2+} in $PbCl_2$.[18]

3. Magnetism in Eu^{2+} Compounds. As usual for Eu^{2+} compounds, the electronic ground state is a well-isolated $J = {}^7/_2$ multiplet, consistent with the paramagnetic moments close to the free-ion value $\mu_{eff} = g_J\mu_B(J(J+1))^{1/2} = 7.94\ \mu_B$ (Table V). The low ordering and paramagnetic Curie temperatures are discussed in terms of the relationship between crystal structure and exchange mechanisms based on extensive discussions in the Eu chalcogenides[2] (Table VI).

In such magnetic insulators, the discussion is safely restricted to nn (J_1) and nnn (J_2) exchange.[34] The J_1 interaction is fer-

(23) Coulthard, M. A. *J. Phys. B* **1973**, *6*, 23.
(24) Zinn, W. *J. Magn. Magn. Mater.* **1976**, *3*, 23.
(25) Baberschke, K. *Z. Phys.* **1973**, *252*, 65.
(26) Kropp, H.; Zipf, W.; Dormann, E.; Buschow, K. H. J. *J. Magn. Magn. Mater.* **1979**, *13*, 224.
(27) Kalvius, G. M.; Shenoy, G. K. *Z. Naturforsch., A* **1971**, *26A*, 353.
(28) See e.g.: Mössbauer Isomer Shifts"; Shenoy, G. K., Wagner, F. E., Eds.; North-Holland Publishing Co.: Amsterdam, 1978.
(29) Friedt, J. M.; Danon, J. In "Modern Physics in Chemistry"; Fluck, E., Goldanskii, V. I., Eds.; Academic Press: New York, 1979; pp 195–320.
(30) Sanderson, R. T. *J. Am. Chem. Soc.* **1983**, *105*, 2259.
(31) Arlman, E. J. *Recl. Trav. Chim. Pays-Bas* **1968**, *87*, 1217.
(32) Sauer, C.; Köbler, U.; Zinn, W.; Kalvius, G. M. *J. Phys.* (*Orsay, Fr.*) *Collloque C6* **1974**, *35*, 269.
(33) Petzel, T.; Greis, O. *Z. Anorg. Allg. Chem.* **1973**, *396*, 95.

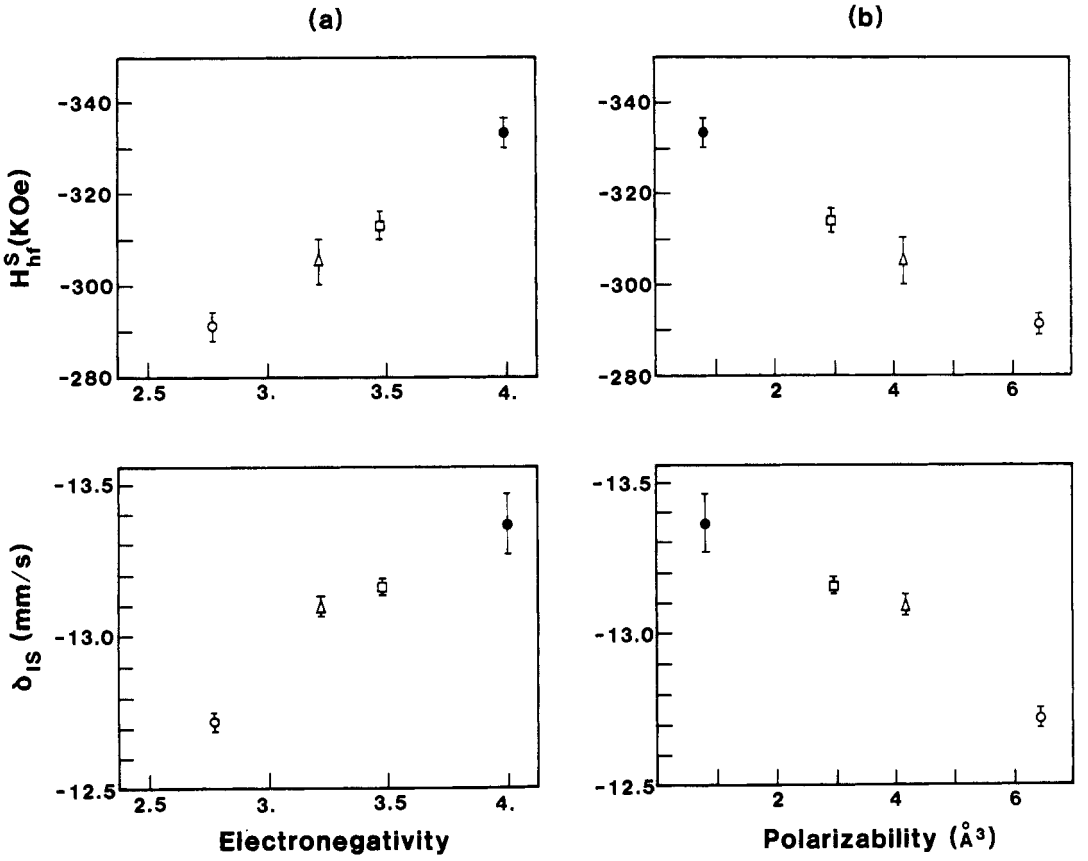

Figure 10. Correlation between the hyperfine parameters δ_{IS} and H_{hf}^S and the ligand electronegativity[30] (a) and the ligand polarizability[31] (b): ●, EuF_2; □, $EuCl_2$; △, $EuBr_2$; ○, EuI_2.

Table VI. Crystallographic Data of EuX_2 Relevant to Their Magnetic Behavior[a]

	no. of nn Eu	d(Eu-Eu) (nn), Å	∠Eu-X-Eu (nn), deg	no. of nnn Eu	d(Eu-Eu) (nnn), Å	∠Eu-X-Eu (nnn), deg
EuF_2	12	4.13	109.5	6	5.84	
$EuCl_2$	12	4.48-5.02	82-118	4	6.35	154
$EuBr_2$ Eu(1)	8	4.56-5.09	86-108	4	6.05	152
$EuBr_2$ Eu(2)	9	4.56-5.09	86-110	5	6.01-6.36	139-152
EuI_2	7	4.86-5.50	93-108	4	6.15-6.36	142

[a] Key: nn = nearest neighbor; nnn = next nearest neighbor.

romagnetic and arises from the direct transfer of 4f electrons to a 5d orbital of a nn Eu ion. The J_2 interaction corresponds to three competing mechanisms,[3] i.e. (i) the usual Kramers–Anderson superexchange (being antiferromagnetic), (ii) indirect f–d exchange via overlap of Eu 5d and anion p orbitals (being antiferromagnetic), and (iii) a (ferromagnetic) cross-term between the above two mechanisms. The second component of J_2 is generally determinant in the Eu chalcogenides, except for EuO where J_2 is ferromagnetic. In view of the difficulty of discussing J_2 a priori, this term is accepted as constantly antiferromagnetic along the halide series. The above considerations allow prediction of enhancement of J_1, i.e. promotion of ferromagnetism, under the condition of a large 4f–5d overlap between nn Eu atoms. This will arise as a consequence of combined small Eu interatomic distances and appropriate crystal field splitting of the 5d orbital such as to promote overlap with the 4f orbital.

The latter effect is illustrated by comparing antiferromagnetic EuF_2 (T_t = 1.0 K) with ferromagnetic EuS (T_t = 16.6 K). Indeed, the Eu interatomic distances are comparable (4.13 and 4.22 Å in EuF_2 and EuS, respectively), but the crystal field splittings of the 5d orbital are different as a result of cubic and octahedral coordinations, respectively. The 5d t_{2g} crystal field multiplet lies lowest in EuS, hence favoring orbital overlap and consequently ferromagnetic (J_1) nn interaction. On the opposite side, low ordering temperature and antiferromagnetism in EuF_2 can be assigned to reduced J_1 because the 5d t_{2g} sublevel is at higher energy, thus reducing the 4f–5d nn overlap. Also, the Curie temperatures in the ferromagnets EuH_2 and EuS are close (T_t = 18.3 and 16.6 K, respectively) in spite of shorter average Eu interatomic distances in EuH_2 (3.94 vs. 4.22 Å in EuS); this is assigned to the lower symmetry of the crystal structure of EuH_2 that reduces J_1 because the direct Eu overlap is restricted to 10 among the 12 nn Eu atoms.[35]

From extrapolation of the above systematics to the Eu dihalides, it is suggested that the low ordering temperatures observed for $EuCl_2$ and EuI_2 (as well as the paramagnetism of $EuBr_2$ down to 1.1 K) arise primarily from the relatively large Eu interatomic distances (i.e., slightly larger than for instance in EuTe, 4.67 Å), in addition to the effect of low site symmetry. These factors consistently weaken the ferromagnetic exchange J_1. Moreover, the nnn interactions are weakened by bonding angles Eu–X–Eu deviating largely from 180° (Table VI). These considerations account qualitatively for the reduced ordering temperatures in comparison to the chalcogenides and for the variety of magnetic

(34) Bohn, H. G.; Zinn, W.; Dorner, B.; Kollmar, A. *Phys. Rev. B: Condens. Matter* **1980**, *22*, 5447.

(35) Bischof, R.; Kaldis, E.; Wachter, P. *J. Magn. Magn. Mater.* **1983**, *31–34*, 255.

ground states observed in the Eu dihalides.

Summary and Conclusions

The structural, electronic, and magnetic properties of europium dihalides are established from the combination of X-ray diffraction, magnetic susceptibility, and ^{151}Eu Mössbauer spectrometry results. The bonding properties, i.e. the charge and spin densities at the Eu nucleus, are inferred from the isomer shift and hyperfine field, respectively. The evolution of these parameters along the series of compounds reveals a correlated dependence, which indicates covalency effects involving primarily the Eu 6s valence orbital being populated by charge transfer from the ligand s (or p) orbitals. The relatively large Eu interatomic distances and the low symmetry of the Eu sites account qualitatively for the low ordering temperatures (in comparison to other Eu^{2+} insulators) measured for $EuCl_2$ and EuI_2 ($T_t \leq 1.8$ K) and the paramagnetism of $EuBr_2$ down to 1.1 K.

Acknowledgment. We gratefully acknowledge the skillful technical contributions by W. Kuhn and A. Bonnenfant.

Contribution from the School of Chemistry, University of Sydney, Sydney, N.S.W. 2006, Australia, and Department of Inorganic Chemistry, University of Melbourne, Parkville, Victoria 3052, Australia

Ultrasonic Relaxation and Variable-Pressure Spectrophotometric Study of the Planar ⇌ Octahedral Equilibrium in Aqueous Solutions of [[1*R*,4*S*,8*S*,11*R*]-1,4,8,11-Tetramethyl-1,4,8,11-tetraazacyclotetradecane]nickel(II) Perchlorate, Ni(Me$_4$cyclam)(ClO$_4$)$_2$ (*trans*-III Isomer)

JAMES K. BEATTIE,*[1a] M. TERRY KELSO,[1a] WAYNE E. MOODY,[1a] and PETER A. TREGLOAN[1b]

Received January 6, 1984

A single relaxation curve describes the excess ultrasound adsorption in aqueous solutions of the title compound, Ni(Me$_4$cyclam)(ClO$_4$)$_2$. The relaxation time at 25 °C of 16.8 ± 0.1 ns is identified as arising from perturbation of the equilibrium between the diamagnetic planar complex and the paramagnetic octahedral complex formed by trans addition of two water molecules. From equilibrium constants K_{46} determined by the Evans NMR method, rate parameters at 25 °C were calculated: $k_{46} = 3.10 \times 10^7$ s^{-1}, $\Delta H_{46}^{\ddagger} = 2.44$ (2) kcal mol^{-1}, $\Delta S_{46}^{\ddagger} = -16.06$ (3) cal deg^{-1} mol^{-1}; $k_{64} = 2.85 \times 10^7$ s^{-1}, $\Delta H_{64}^{\ddagger} = 9.31$ (2) kcal mol^{-1}, $\Delta S_{64}^{\ddagger} = 6.79$ (1) cal deg^{-1} mol^{-1}. From the relaxation amplitude, the volume difference $\Delta V_{46}°$ is found to be −10.1 (2) cm^3 mol^{-1}. An independent measurement from the pressure dependence of the electronic absorption spectrum gives −8.6 (3) cm^3 mol^{-1}. For Ni(cyclam)$^{2+}$, the analogous relaxation time is somewhat longer and the volume change measured from the pressure dependence of the electronic spectrum only −3.5 (1) cm^3 mol^{-1}.

Introduction

The existence of a diamagnetic–paramagnetic equilibrium in aqueous solutions of the *trans*-III isomer of the tetramethylcyclam complex of nickel(II) [[1*R*,4*S*,8*S*,11*R*]-1,4,8,11-tetramethyl-1,4,8,11-tetraazacyclotetradecane]nickel(II), Ni(Me$_4$cyclam)$^{2+}$ (*trans*-III isomer)) was suggested when the complex was first prepared.[2] Recently, the thermodynamics of the equilibrium have been measured with visible electronic absorption spectra,[3] solution magnetic susceptibility (Evans method),[3] and proton NMR contact shifts.[4] From the solution electronic spectrum it has been inferred[3] that the paramagnetic form is octahedrally coordinated with two solvent molecules:

$$\text{Ni(Me}_4\text{cyclam)}^{2+} + 2\text{H}_2\text{O} \underset{}{\overset{K_{46}}{\rightleftharpoons}} \text{Ni(Me}_4\text{cyclam)(H}_2\text{O)}_2^{2+} \quad (1)$$

The dynamics of this equilibrium have not been described for aqueous solutions, although related processes in acetonitrile have been studied in detail.[5,6]

We have used an ultrasonic relaxation technique to obtain the relaxation time for equilibrium 1 and have independently measured the equilibrium constant by using the Evans NMR method. With these data, the rate constants k_{46} and k_{64} have been calculated, along with a value for the volume change associated with the equilibrium. Good agreement was found with the volume change measured directly with high-pressure spectrophotometry and also with that reported[4] from high-pressure NMR measurements. Some observations were also made on the analogous equilibrium of the cyclam complex of nickel(II) ([1,4,8,11-tetraazacyclotetradecane]nickel(II), Ni(cyclam)$^{2+}$).[3,7-9]

Experimental Section

The perchlorate salts of the complexes were prepared by methods described in the literature[2,10,11] from cyclam ligand purchased from Strem Chemicals Inc. Ultrasonic absorption measurements were made as described previously.[12,13] Solution magnetic susceptibility measurements of 0.020 g mL^{-1} of Ni(Me$_4$cyclam)(ClO$_4$)$_2$ in H_2O by the Evans method were made at 90 MHz (Bruker HX-90). An internal reference of 5% v/v *t*-BuOH was used. A capillary of ethylene glycol was used as an internal temperature probe. The data were corrected for changes in density and, hence, concentration with changes in temperature.[13]

(1) (a) University of Sydney. (b) University of Melbourne.
(2) Wagner, F.; Barefield, E. K. *Inorg. Chem.* **1976**, 15, 408. The *trans*-III nomenclature was defined in: Bosnich, B; Poon, C. K.; Tobe, M. L. *Inorg. Chem.* **1965**, *4*, 1102.
(3) Herron, N.; Moore, P. *Inorg. Chim. Acta* **1979**, *36*, 89.
(4) Merbach, A. E.; Moore, P.; Newman, K. E. *J. Magn. Reson.* **1980**, *41*, 30.
(5) Herron, N.; Moore, P. *J. Chem. Soc., Dalton Trans.* **1979**, 441.
(6) Helm, L.; Meier, P.; Merbach, A. E.; Tregloan, P. A. *Inorg. Chim. Acta* **1983**, *73*, 1.
(7) Anichini, A.; Fabbrizzi, L.; Paoletti, P.; Clay, R. M. *Inorg. Chim. Acta* **1977**, *24*, L21.
(8) Vigee, G. S.; Watkins, C. L.; Bowen, H. F. *Inorg. Chim. Acta* **1979**, *35*, 255.
(9) Pell, R. J.; Dodgen, H. W.; Hunt, J. P. *Inorg. Chem.* **1983**, *22*, 529.
(10) Wagner, F.; Mocella, M. T.; D'Aniello, M. J., Jr.; Wang, A. H.-J.; Barefield, E. K. *J. Am. Chem. Soc.* **1974**, *96*, 2625.
(11) Bosnich, B.; Tobe, M. L.; Webb, G. A. *Inorg. Chem.* **1965**, *4*, 1109.
(12) Beattie, J. K.; Binstead, R. A.; West, R. J. *J. Am. Chem. Soc.* **1978**, *100*, 3044.
(13) Binstead, R. A.; Beattie, J. K.; Dewey, T. G.; Turner, D. H. *J. Am. Chem. Soc.* **1980**, *102*, 6442.

0020-1669/85/1324-0415$01.50/0